UNSTEADY CONVECTIVE DIFFUSION IN VISCOELASTIC FLUID FLOWING THROUGH A TUBE

D. C. Dalal and B. S. Mazumder

Physics and Applied Mathematics Unit, Indian Statistical Institute, Calcutta 700035, India

(*Received September* 1995; *in revised form September* 1996)

Abstract The longitudinal dispersion of passive contaminant molecules released in unsteady viscoelastic fluid flowing through a tube is examined. A finite difference implicit scheme is adopted to solve the Aris integral moment equations arising from the unsteady convective–diffusion equation for all time period. Here it is shown how the injected material spread due to the shear effect in the viscoelastic fluid caused by the combined action of periodic flow and lateral diffusion about its mean position, centre of gravity of mass moves and the mean concentration distribution approaches to Gaussianity, when the contaminant is initially uniform over the cross-section of the tube and the Péclet number is large. The analysis reveals that for viscoelastic fluid the dispersion coefficient changes cyclically with a double frequency period and reaches asymptotically a stationary state after a certain time as in the case of a Newtonian fluid, and its increases with the viscoelastic parameter. Further, it shows that there is a remarkable similarity between the mean concentration distribution of solute in a Newtonian and non-Newtonian fluid.

Keywords: longitudinal dispersion, non-Newtonian fluid, viscoelastic fluid, oscillatory flow, finite-difference scheme

1. INTRODUCTION

The study of dispersion of contaminants in a fluid is a part of Environmental Fluid Mechanics which has become essential in controlling pollution of rivers, environment, etc. due to the release of contaminating materials from different sources. Now-a-days this study, which gives an insight into dispersion phenomena of passive contaminants in solvents, has primary importance in industrial and technological fields.

In his classic paper, Taylor [1] pointed out that in longitudinal dispersion of soluble matter in a moving fluid, solute is more slowly dispersed by molecular or turbulent diffusion alone than the dispersion due to 'shear effect' caused by combined effects on convection and lateral diffusion. Aris [2] subsequently proposed an idea of moment method in solving the model removing the restrictions imposed by Taylor and studied the asymptotic behaviour of second moment about the mean. Barton [3] resolved certain technical difficulties in Aris' method and obtained the solutions of second and third moment equations of the distribution of solute which are valid for all time. All the work mentioned above was based on steady flow.

The longitudinal dispersion of a solute in time-dependent flow due to periodic pressure gradient in an infinite tube was first studied by Aris [4] using his method of moments, and his analysis was limited to asymptotically large time after the injection of the solute. Mukherjee and Mazumder [5] extended the Aris–Barton theory for studying the all-time evolution of the second central moment of dispersion of passive contaminant in the shearing current due to the combined effect of steady and periodic flows within a conduit of uniform cross-section. The solution was based on the method of separation of variables, which depends on a certain eigenvalue problem with a discrete spectrum of eigenvalues. Mazumder and Das [6] extensively studied the effect of boundary absorption on the axial dispersion of contaminant cloud released in pulsatile tube flow. Using a numerical scheme they computed the effective diffusivity for different values of absorption parameter for all time periods. The problem of dispersion phenomenon in time-dependent flows within conduits has been studied by Chatwin [7], Smith [8], Jimenez and Sullivan [9], Yasuda [10], Mazumder and Das [11] and others.

Fan and Hwang [12] first extended the analysis of Taylor to the dispersion of solute in non-Newtonian (Ostwald–de Waele) fluid and they showed that Taylor's method can be applied in the case of non-Newtonian fluid. Fan and Wang [13] also studied Taylor's analysis of dispersion in the flow of a Bingham plastic and an Ellis model fluid and showed that Aris' modification of Taylor's analysis can be applied in the case of non-Newtonian fluid. Using the Taylor conceptual model, Erdoğan [14] studied the dispersion in non-Newtonian flow at low flow rates. He showed that the longitudinal dispersion coefficient depends on the ratio of the yield stress to the wall stress. When the ratio is zero it is equivalent to a Newtonian fluid. For a ratio greater than zero, the dispersion coefficient first increases and then decreases with the increase of the ratio, and the longitudinal dispersion coefficient becomes zero when the value of the ratio reaches 1. He also studied the effect of a Bingham plastic and Ostwald–de Waele fluids on dispersion and observed that initially the dispersion coefficient increases upto a certain value and then it decreases with an increase in the non-Newtonian parameter. Dispersion in Eyring and Reiner Philippoff model fluids has been studied by Ghoshal [15] using Taylor's analysis but he did not discuss anything in dispersion phenomenon as in his study some integrals were unevaluated. Shah and Cox [16] and Gupta and Mazumder [17] solved the problem completely and showed that the dispersion coefficient decreases with the increase of the Eyring model parameter. However, all the investigations on non-Newtonian fluid models mentioned above were asymptotically valid for a large time after the injection of the solute. Subramanian and Gill [18] explored the generalized dispersion model valid for all time period to study the spreading of solutes in non-Newtonian fluid (Ostwald–de Waele), but they confined their analysis to the steady laminar flow in a tube. They found that the dispersion coefficient at any given time decreases with increasing the non-Newtonian parameter.

To the best of our knowledge, the dispersion of a solute in oscillating flow of a viscoelastic fluid has not been studied in the literature. Our main objective of the present paper is to explore the dispersion phenomenon of a solute in Maxwell linear model of viscoelastic fluid (Bird *et al.* [19]) within a tube when the flow is oscillatory due to the periodic pressure gradient. More precisely, it is shown for all time period how the spreading of tracers is influenced by the combined action of characteristic relaxation time and the frequency of oscillation about the mean position, the center of mass of slug moves and the behaviour of mean concentration distributions approaches to normality, when the contaminant is initially uniform over the cross-section of the tube and the Péclet number is large. The motivation of the study of viscoelastic oscillatory flows stems mainly from the important application, namely the dispersion of tracers in pulsatile blood streams and the mass transfer in polymer solutions. In particular, a water-solution of polyacrylamide is a well-known viscoelastic fluid.

2. MATHEMATICAL FORMULATION

If the convected derivative is written in full then the constitutive equation of the Maxwell model of a viscoelastic fluid which is a superposition of the Hookean solid and Newtonian liquid with zero retardation time is given by (Oldroyd [20]),

$$\tau_{ij} + t_0 \left(\frac{\partial \tau_{ij}}{\partial t'} + u'^k \tau_{ij,k} + u'^k_{,i} \tau_{kj} + u'^k_{,j} \tau_{ik} \right) = -\mu (u'_{i,j} + u'_{j,i}) \tag{1}$$

Here t_0 is a characteristic relaxation time for the fluid, u'_i is the velocity in the ith direction, μ is the coefficient of viscosity of the fluid, and τ_{ij} is the shear stress.

Consider an oscillatory fully developed incompressible laminar flow of the above fluid in a straight circular pipe with uniform cross section of radius R. As the flow is induced by the periodic pressure difference along the axial direction, the flow will be unidirectional. So the velocity has only axial component u'_z, depending on radial coordinate r and time t. Also the stresses have r–z component τ_{rz} only. Taking this into account further simplification is possible if we take the linearized equation as well as if we consider slow motion of the fluid. So the proper invariant derivative in equation (1) reduces to the partial time derivative.

Neglecting the convective term $u' \cdot \nabla u'$ of the momentum equation, the linearized equation of motion in two-dimensional cylindrical form is given by, (see Bird *et al.* [19])

$$\rho \frac{\partial u_z'}{\partial t'} = -\frac{\partial p'}{\partial z'} - \frac{1}{r'}\frac{\partial}{\partial r'}(r'\tau_{rz}) \tag{2}$$

and linearized Maxwell model is

$$\tau_{rz} + t_0 \frac{\partial \tau_{rz}}{\partial t'} = -\mu \frac{\partial u_z'}{\partial r'} \tag{3}$$

where ρ is the density of the fluid, p' is the pressure and $t_0 = \mu/G$, G is the modulus of shear rigidity.

Eliminating τ_{rz} from equations (2) and (3) we have

$$\rho t_0 \frac{\partial^2 u_z'}{\partial t'^2} + \rho \frac{\partial u_z'}{\partial t'} = -t_0 \frac{\partial^2 p'}{\partial t' \partial z'} - \frac{\partial p'}{\partial z'} + \mu \frac{1}{r'}\frac{\partial}{\partial r'}\left(r' \frac{\partial u_z'}{\partial r'}\right) \tag{4}$$

The boundary conditions are,

$$u' = 0 \quad \text{at} \quad r' = R \tag{5}$$

and the velocity at the center of the pipe is finite.

As the flow is oscillatory, velocity and pressure of the fluid can be written as of the following form,

$$u_z' = \text{Real}\{u_0(r)e^{i\omega t'}\}, \qquad -\frac{\partial p'}{\partial z'} = b_0 \,\text{Real}\{e^{i\omega t'}\} \tag{6}$$

Using the expression of (6), the solution of equation (4) subject to the boundary condition (5) for periodic flow is:

$$u_z' = \text{Real}\left[\frac{b_0}{i\omega\rho}\left(1 - \frac{J_0(kr')}{J_0(kR)}\right)e^{i\omega t'}\right] \tag{7}$$

where, $k^2 = -i\omega\rho(1 + i\omega t_0)/\mu$, and ω is frequency of oscillation when the local fluid motion is a sinusoidal function.

The velocity from equation (7) can be written in dimensionless form as:

$$u = -\text{Real}\left[\frac{i}{\alpha}\left\{1 - \frac{J_0(rk_1)}{J_0(k_1)}\right\}e^{i\alpha S t}\right], \tag{8}$$

where $k_1 = \sqrt{-i\alpha(1 + \alpha T_0)}$, $\alpha = \omega R^2/\nu$ is the dimensionless oscillation Reynolds number or frequency parameter, $S = \nu/D$ is the Schmidt number, $T_0 = \nu t_0/R^2$ is the dimensionless elasticity parameter, $u_z = u_z'/U$ is axial velocity in which $U = R^2 b_0/\mu$ is the time averaged velocity, and $r = r'/R$ is the dimensionless radial distance. If the dimensionless elasticity number T_0 is zero, the velocity equation (8) corresponds to the oscillatory Newtonian fluid flow through a tube (Uchida [21], Schlichting [22]). The oscillating flow of a viscoelastic fluid is characterized by dimensionless number α, S and T_0. Here $\alpha = \omega R^2/\nu$ is a measure of the ratio of time necessary for shear-wave propagation across the tube section to the period of oscillation or the ratio of pipe radius to the Stokes-layer thickness. The Schmidt number S is the ratio of viscous diffusion and molecular diffusion; and αS is the measure of the ratio of the characteristic time of transverse diffusion to the period of oscillation. The dimensionless viscoelastic parameter T_0 $(= t_0/(R^2/\nu))$ is the ratio of the fluid relaxation time to the time taken for shear-wave propagation over the cross-section of the tube. Figure 1(a–d) presents the velocity profiles against the frequency parameter α in different flow phases for various values of T_0, and $r = 0.5$. For a Newtonian fluid ($T_0 = 0$), velocity decreases with increase in α, whereas for a viscoelastic fluid ($T_0 > 0$), it increases upto a certain α, then decreases (Khabakhpasheva *et al.* [23]) for the phases $\alpha St = 0, \pi$. The increase of velocity with viscoelastic parameter T_0 seems to be due to the presence of elasticity in the liquid (Beard and Walters [24]). For phases $\alpha St = \pi/2$, and $3\pi/2$, it is oscillatory in nature upto a certain

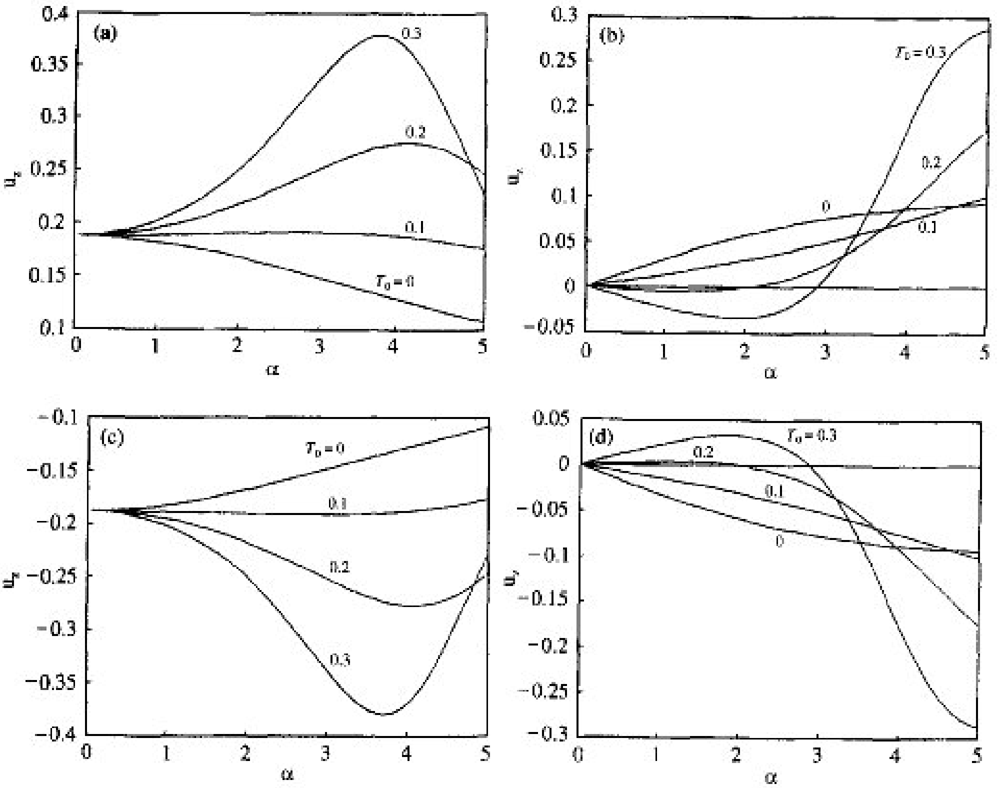

Fig. 1. Oscillatory velocity u_z of a viscoelastic fluid against frequency parameter α for different phase: (a) $\alpha St = 0$, (b) $\alpha St = \pi/2$, (c) $\alpha St = \pi$, (d) $\alpha St = 3\pi/2$, at $r = 0.5$.

value of α, then it increases with increase in T_0 at large α. It may be mentioned here that the velocity profile for a pulsating Poiseuille flow of a non-Newtonian fluid studied by Rajagopal and Sciuba [25] is somewhat consistent with the present velocity profile for a small value of frequency parameter. It is also observed from the figure that the velocity profile in the flow phases is more flattened with deceleration than in the phases with acceleration.

If a slug is released in the above mentioned periodic flow in a tube, the concentration $C(t, r, z)$ of the solute, with constant molecular diffusivity D, satisfies the non-dimensional convective–diffusion equation of the form

$$\frac{\partial C}{\partial t} + \mathrm{Pe}\, u_z \frac{\partial C}{\partial z} = \left[\frac{1}{r}\frac{\partial}{\partial r}\left(r\frac{\partial C}{\partial r}\right) + \frac{\partial^2 C}{\partial z^2}\right] \tag{9}$$

where $z = z'/R$ and $\mathrm{Pe} = RU/D$, $u_z = u_z'/U$, $t = Dt'/R^2$, $r = r'/R$. Here u_z is the periodic velocity due to imposed periodic pressure gradient, U is the reference velocity, and Pe, the Péclet number is the ratio of the characteristic time of the diffusion process (R^2/D) to the convective process (R/U).

The initial and boundary conditions are

$$\left.\begin{aligned}
&C(0, r, z) = \delta(z),\\
&\frac{\partial C}{\partial r} = 0 \text{ at } r = 1,\\
&C \text{ finite at all points},\\
&z^m \frac{\partial^n C}{\partial z^n} \to 0 \text{ as } |z| \to \infty \text{ for } m, n = 0, 1, 2, \ldots,\\
&\frac{1}{\pi}\int_0^1 \int_0^{2\pi} \int_{-\infty}^{\infty} rC(0, r, z)\, \mathrm{d}r\, \mathrm{d}\theta\, \mathrm{d}z = 1,
\end{aligned}\right\} \tag{10}$$

where $\delta(z)$ is the Dirac delta function.

Following the Aris [2] method of moments, the pth integral moment of the concentration distribution can be defined as

$$C_p = \int_{-\infty}^{\infty} z^p C(t, r, z)\,\mathrm{d}z, \tag{11}$$

and

$$M_p = \bar{C}_p = \frac{1}{2\pi}\int_0^{2\pi} \mathrm{d}\theta \int_0^1 r C_p(t, r)\,\mathrm{d}r. \tag{12}$$

So using equations (11) and (12), the diffusion equations (9) and (10) can be written in the form of C_p and M_p separately which are

$$\frac{\partial C_p}{\partial t} - \frac{1}{r}\frac{\partial}{\partial r}\left(r\frac{\partial C_p}{\partial r}\right) = p\,\mathrm{Pe}\,u_z(t, r)C_{p-1} + p(p-1)C_{p-2}, \tag{13a}$$

with

$$C_p(0, r) = 1 \quad \text{and} \quad \frac{\partial C_p}{\partial r} = 0 \quad \text{at} \quad r = 1, \tag{13b}$$

and

$$\frac{\mathrm{d}M_p}{\mathrm{d}t} = p\,\mathrm{Pe}\,\overline{u_z(t, r)C_{p-1}} + p(p-1)\overline{C_{p-2}}, \tag{14}$$

with

$$M_p(0) = 1, \quad \text{for} \quad p = 0, \quad \text{and} \quad M_p = 0 \quad \text{for} \quad p > 0,$$

overbar denotes the cross-sectional mean.

The pth central moment of concentration distribution about the mean can be written as,

$$\nu_p(t) = \frac{1}{\pi}\frac{\int_0^1\int_0^{2\pi}\int_{-\infty}^{\infty} r(z - z_g)^p C(0, r, z)\,\mathrm{d}r\,\mathrm{d}\theta\,\mathrm{d}z}{\iiint C\,\mathrm{d}v}, \tag{15}$$

where

$$z_g = \frac{\iiint zC\,\mathrm{d}v}{\iiint C\,\mathrm{d}v} = \frac{M_1}{M_0}$$

is the centroid or first moment of the solute which measures the location of the centre of gravity of the slug with the mean velocity of the viscoelastic fluid initially located at the source, and M_0 represents the total mass of inert solute in the whole volume of the tube.

Putting $p = 2, 3, 4$ in (15) we get the central moments as,

$$\left.\begin{aligned} \nu_2(t) &= \frac{M_2}{M_0} - z_g^2 \\ \nu_3(t) &= \frac{M_3}{M_0} - 3z_g\nu_2 - z_g^3 \\ \nu_4(t) &= \frac{M_4}{M_0} - 4z_g\nu_3 - 6z_g\nu_2^2 - z_g^4 \end{aligned}\right\} \tag{16}$$

Here ν_2 represents the variance of the distribution of solute about the centre of the slug. Third (ν_3) and fourth (ν_4) central moments represent the symmetry and peakedness of the distribution of the slug about its mean (z_g), respectively. M_is are calculated from equations (13a) and (14).

3. NUMERICAL PROCEDURE

Because of the complexity of the analytical solution of the moment equation (13a) with the expression of u_z given by equation (8) subject to the initial and boundary conditions specified in (13b), it is solved numerically. A finite-difference scheme based on the Crank–Nicholson implicit method has been adopted to study this problem. A marching technique for time has been used in this equation as the initial condition is specified and the derivatives along the marching direction have been replaced by backward differencing with second order accuracy, whereas the third-order accuracy in central differencing along the radial direction has been used for the diffusion term, and the resulting difference scheme becomes implicit. The scheme has been discussed in detail in the work of Mazumder and Das [6, 11]. The derivatives and all the other terms have been written at the mesh point $(i+1, j)$ where $i = 0$ corresponds to the time $t = 0$ and $j = 0$ to the axis of the pipe $r = 0$. The mesh point (i, j) indicates a point where $t = \Delta t \times i$ and $r = \Delta r \times j$. Δt and Δr are the increments of t and r, respectively. The discretized equations are a system of linear algebric equations with a tridiagonal coefficient matrix,

$$P_j C_p(i+1, j+1) + Q_j C_p(i+1, j) + R_j C_p(i+1, j-1) = S_j \tag{17}$$

where

$$P_j = -\frac{1}{2(\Delta r)^2}\left(\frac{1}{2j} + 1\right),$$

$$Q_j = \frac{1}{\Delta t} + \frac{1}{(\Delta r)^2},$$

$$R_j = \frac{1}{2(\Delta r)^2}\left(\frac{1}{2j} - 1\right),$$

and

$$S_j = \frac{1}{\Delta t} C_p(i, j) + \frac{1}{4j(\Delta r)^2}\{C_p(i, j+1) - C_p(i, j-1)\} + \frac{1}{(\Delta r)^2}\{C_p(i, j+1)$$

$$- 2C_p(i, j) + C_p(i, j-1)\} + \frac{p\mathrm{Pe}}{4}\{u(i+1, j) + u(i, j)\}\{C_{p-1}(i+1, j)$$

$$+ C_{p-1}(i, j)\} + \frac{n(n-1)}{2}\{C_{p-2}(i+1, j) + C_{p-2}(i, j)\}$$

and the matrix elements.

The finite-difference form of the initial and boundary conditions are.

$$\left.\begin{aligned} C_p(1, j) &= \begin{cases} 1 & \text{for } p = 0 \\ 0 & \text{for } p \geqslant 1 \end{cases} \\ C_p(i+1, 1) &= C_p(i+1, -1) \end{aligned}\right\} \tag{18}$$

at the axis, and

$$C_p(i+1, N+1) = C_p(i+1, N-1) \tag{19}$$

at the boundary for $p \geqslant 0$, N is the value of j at the boundary.

This tridiagonal coefficient matrix has been solved by the method of the Thomas algorithm with the help of prescribed initial and boundary conditions. The integration for calculation of M_p from equation (14) has been performed employing Simpson's one-third rule. Initially, velocity is computed from equation (8). Using the values of velocity u_z at the grid $(i+1, j)$ in equation (13a), the concentration C_p is calculated at each grid point of computational domain. Finally, with the help of Simpson's one-third rule, M_p is evaluated using the values of u_z and C_p in the corresponding point. The values of the variables can be calculated for all time iteratively in the marching direction. The present scheme is linearly stable for a finite value of n, where $n = \Delta t/(\Delta r)^2 = 0.01$ because of its implicitness. For frequency parameter $\alpha = 0.5, 4.0$ in oscillatory flow, mesh size has been taken as $\Delta t = 0.00001$ and $\Delta r = 0.01$, and it gives a good accuracy and no considerable difference in results for smaller mesh size.

4. DISCUSSION OF RESULTS

In order the validate the numerical scheme, the values of C_1 and M_1 have been calculated analytically using the moment method and numerically using the present scheme. The first moment of concentration distribution of solute C_1 has been studied from equation (13a). So the diffusion equation for C_1 is

$$\frac{\partial C_1}{\partial t} - \frac{1}{r}\frac{\partial}{\partial r}\left(r\frac{\partial C_1}{\partial r}\right) = \mathrm{Pe}\, u_z C_0$$

This is a one-dimensional diffusion equation having a source term $\mathrm{Pe}\, u_z C_0$. The first moment C_1 can easily be solved using the method given by Mukherjee and Mazumder [5] and the expression for C_1 is given by,

$$C_1(r,t) = \mathrm{Real}\left[\frac{2i\mathrm{Pe}}{\alpha}\frac{k_1 J_1(k_1)}{J_0(k_1)}\sum_j \frac{J_0(\alpha_j r)}{(k_1^2-\alpha_j^2)(\alpha_j^2+i\alpha S)\,J_0(\alpha_j)}\{e^{i\alpha St}-e^{-\alpha_j^2 t}\}\right.$$
$$\left. -\frac{\mathrm{Pe}}{\alpha^2 S}\left\{1-\frac{2J_1(k_1)}{k_1 J_0(k_1)}\right\}\{e^{i\alpha St}-1\}\right], \tag{20}$$

where J_0, J_1 are the 1st kind Bessel functions of zeroth and first order respectively. α_js are the zeros of J_1.

The values of C_1 calculated from the numerical scheme as well as from the analytical method given by Mukherjee and Mazumder [5] have been compared and it is found that the analytical and numerical values are in good agreement. The variation of distribution of C_1 against r for different phase values has been plotted in Fig. 2 for $T_0 = 0.1, 0.3$ and

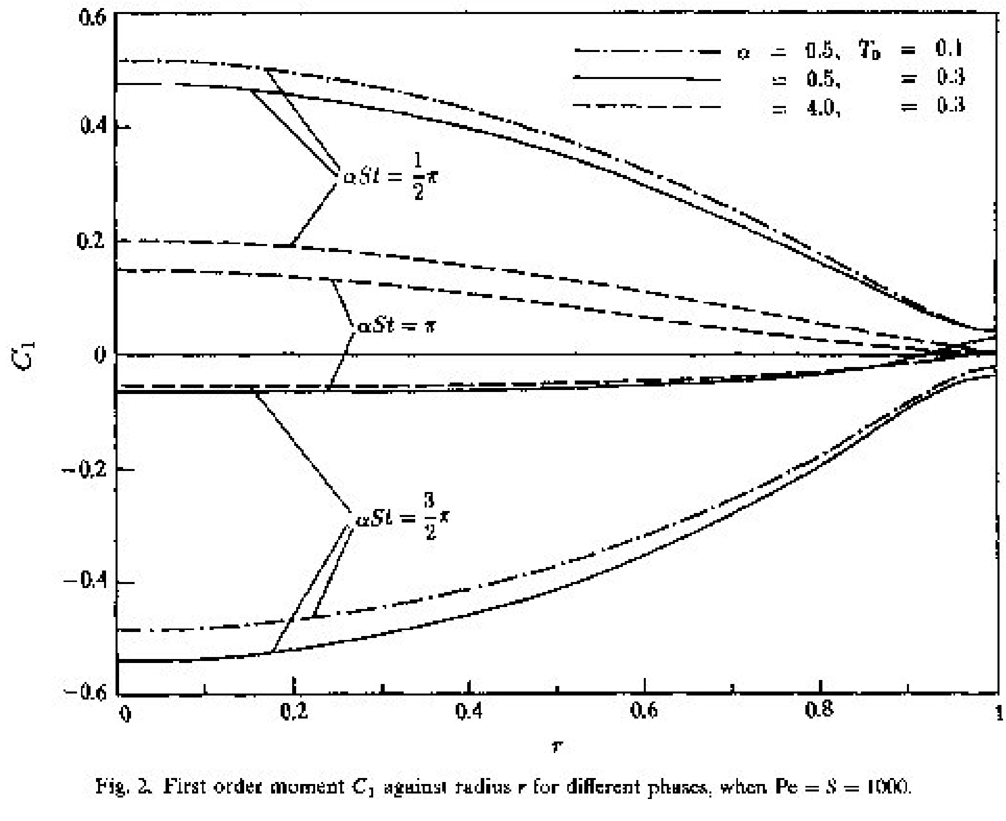

Fig. 2. First order moment C_1 against radius r for different phases, when $\mathrm{Pe} = S = 1000$.

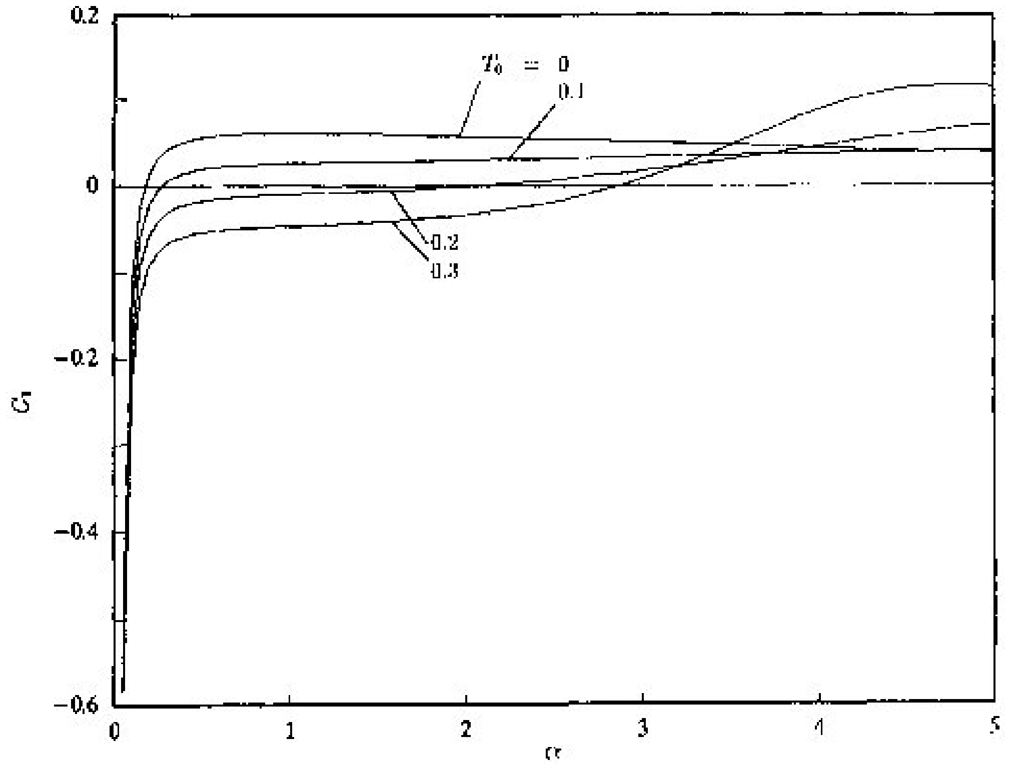

Fig. 3. First order moment C_1 against frequency parameter α, when Pe = S = 1000 and $r = 0.5$ for $\alpha St = \pi$.

$\alpha = 0.5, 4.0$. C_1 reveals its periodicity with flow phases because of the oscillatory nature in velocity u_z. Figure 3 shows the variation of C_1 against α for different values T_0, $r = 0.5$, and $\alpha St = \pi$. It is interesting to note that in the case of a Newtonian fluid ($T_0 = 0$) the effect of the frequency parameter α on C_1 is not significant, whereas with the increase of the visco-elastic parameter $T_0 > 0$, C_1 decreases for a certain range of α, then it increases.

The first moment M_1 indicates the mean concentration distribution over the cross-section of the tube. Putting $p = 1$, the equation of M_p gives,

$$\frac{dM_1}{dt} = \text{Pe}\, \overline{u_z C_0},$$

with $M_1(0) = 0$

Similar to C_1, M_1 can be obtained as

$$M_1(t) = -\frac{\text{Pe}}{\alpha^2 S}\text{Real}\left[\left\{1 - \frac{2J_1(k_1)}{k_1 J_0(k_1)}\right\}\{e^{i\alpha St} - 1\}\right] \tag{21}$$

The mean longitudinal displacement Z_g ($= M_1/M_0$) of the solute moving with the mean periodic velocity of the solvent mainly depends on α, T_0 and t. Figure 4(a, b) shows the displacement of centroid (z_g) for different values of T_0 and $\alpha = 0.5, 4.0$. It is seen that the centroid of the slug moves cyclically with the oscillatory nature of the flow, and it changes asymptotically over a period. For low frequency of oscillation ($\alpha = 0.5$), the amplitude of oscillation decreases in the first part of the period and increases in the second part with the increase in elastic parameter T_0, whereas for a large frequency ($\alpha = 4.0$), the amplitude of oscillation increases in the both parts [Fig. 4(b)]. For both low and high values of frequency, it is seen that there is a phase shift which decreases with an increase in T_0. It is also observed that the amplitude of positive pulsation is more prominent than that of negative pulsation for high frequency.

Owing to the complexity of analytical solution of equations (13a)–(14) for $p = 2$, subject to the initial and boundary conditions, we have solved numerically, and hence the variance

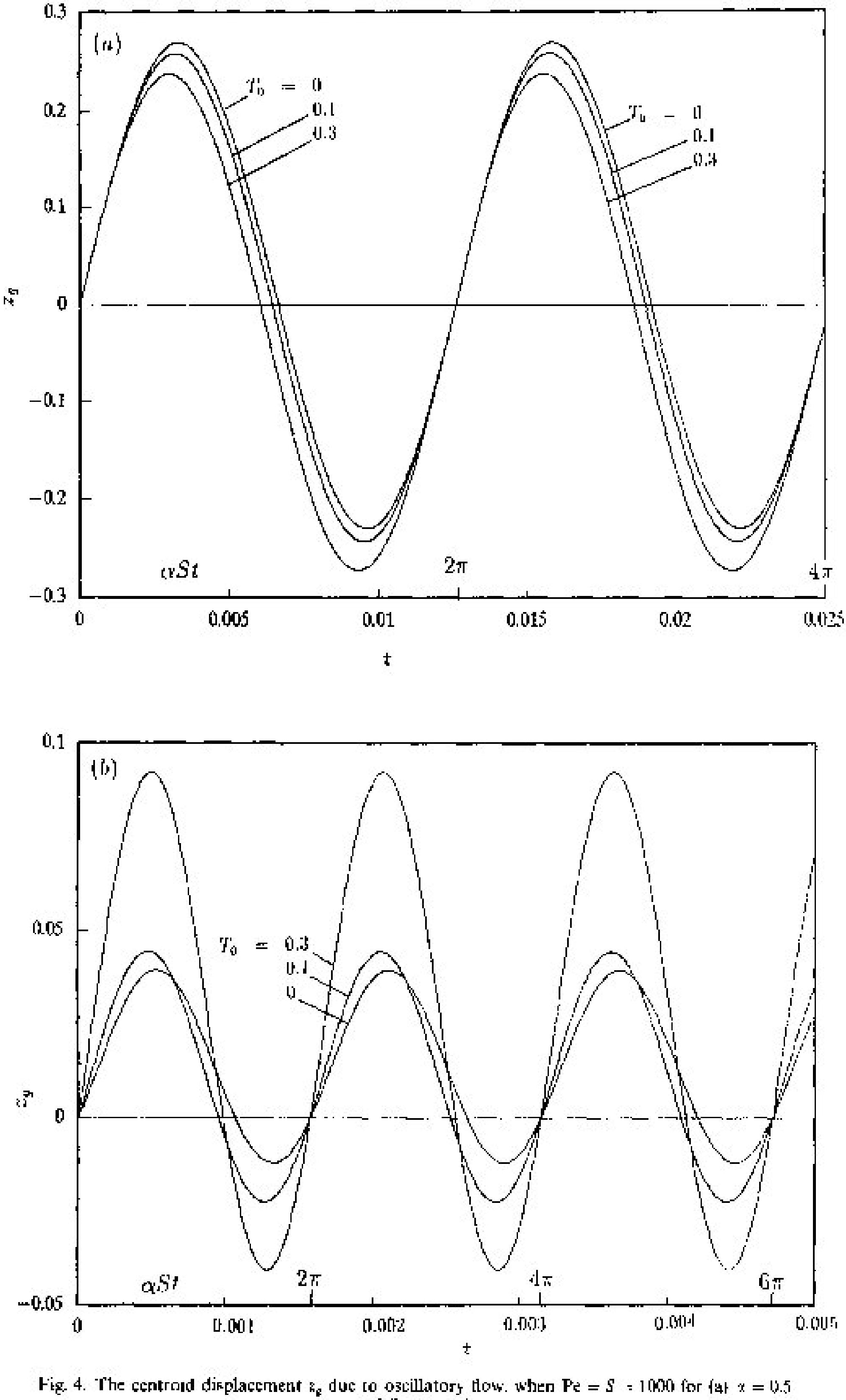

Fig. 4. The centroid displacement z_g due to oscillatory flow, when Pe = S = 1000 for (a) $\alpha = 0.5$ and (b) $\alpha = 4.0$.

v_2 and dispersion coefficient due to shear effect have been evaluated. The plots of second central moment v_2 (variance) of the longitudinal concentration distribution against dispersion time t for $T_0 = 0, 0.1, 0.3$, Pe $= S = 10^3$ have been presented in Fig. 5 when $\alpha = 0.5$ and in Fig. 6 when $\alpha = 4.0$. It is essentially the dispersion due to both the longitudinal diffusion

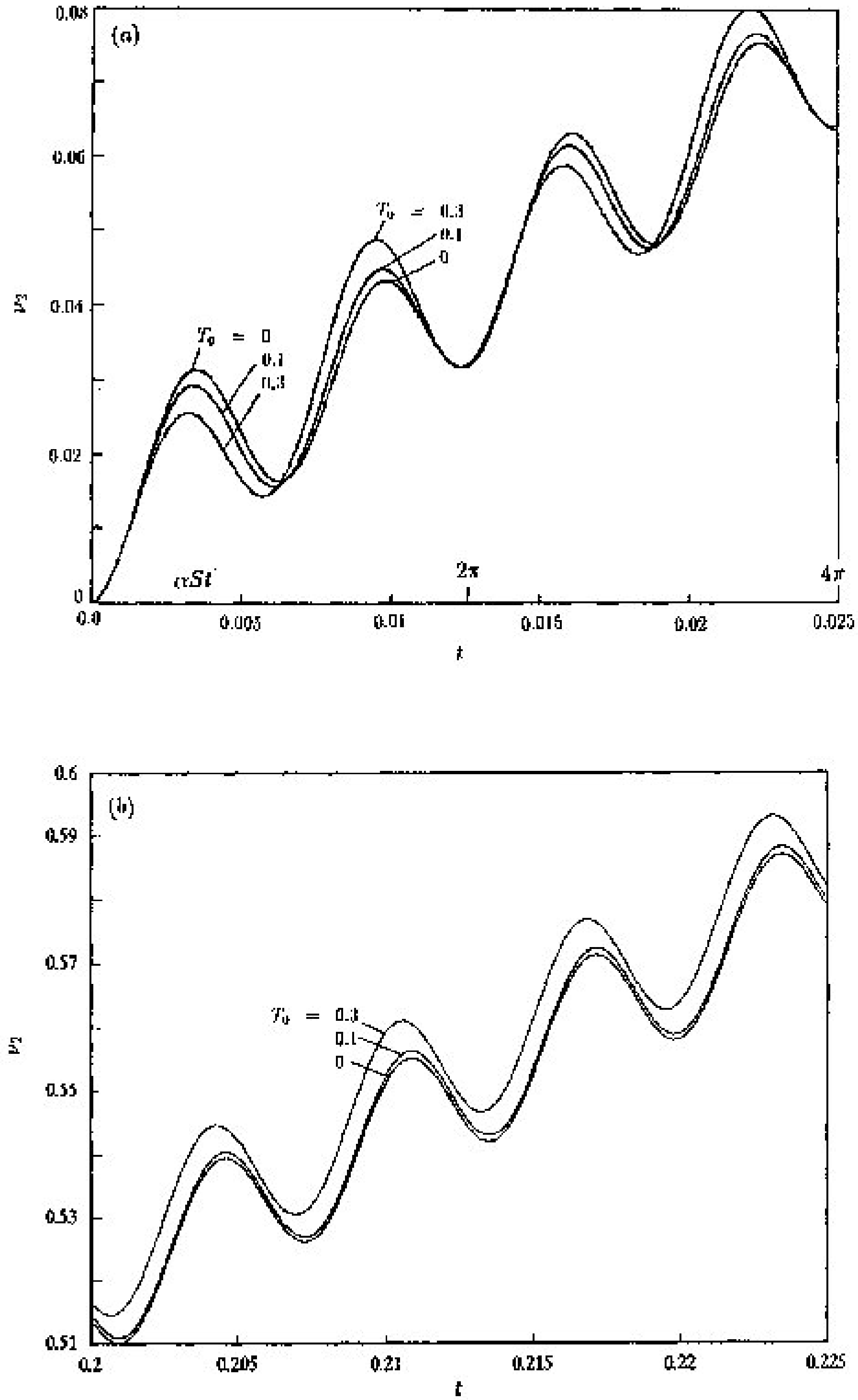

Fig. 5. The temporal variation of variance v_2 for (a) small time, (b) large time, when Pe = S = 1000, α = 0.5.

and interaction of the periodic current and lateral diffusion. At low frequency of oscillation, Fig. 5 shows that for a given value of T_0, the variance increases with time in a wavy pattern. In a complete period, variance decreases in the first part of oscillation, and then increases in the second part with increase in relaxation time T_0 [Fig. 5(a)], but this behaviour completely diminishes for large time where variance increases at a fairly uniform rate with T_0 [Fig. 5(b)]. The increase of variance (v_2) about the mean (z_g) with T_0 can directly be related to the increase of fluid velocity with elasticity in fluid. It also reveals that with an increase of α (i.e. increase of frequency of oscillation) the variance of distribution decreases. For α = 0.5

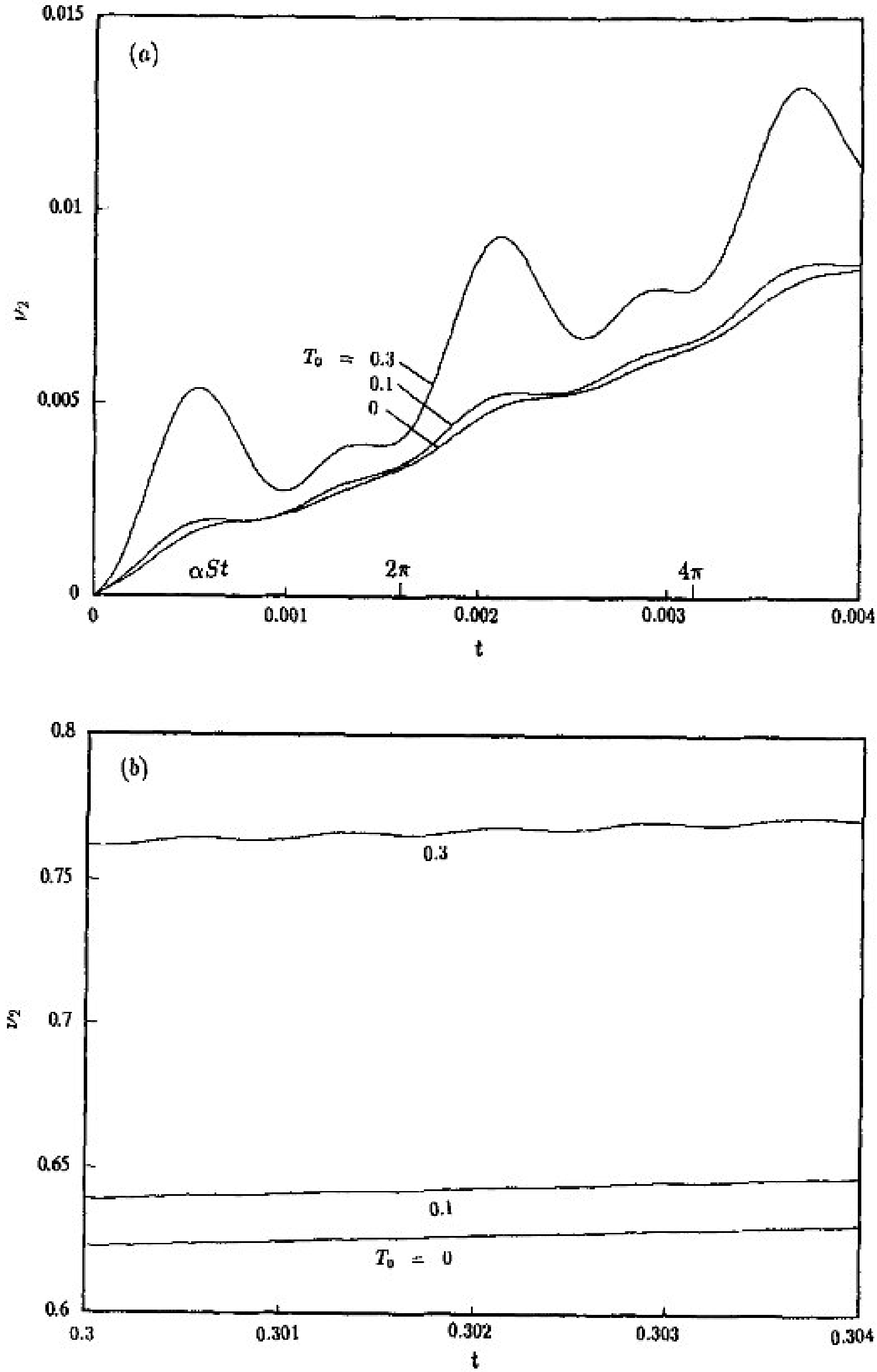

Fig. 6. As Fig. 5 but $\alpha = 4.0$.

the wavy nature of the variance (ν_2) of the solute distribution is almost the same for all time period, whereas for $\alpha = 4.0$ (Fig. 6) it shows double frequency oscillation in a complete period upto a certain time, and it reaches asymptotically a steady state for large time. Further, it may be mentioned here that the amplitude of variance increases for all time period with the relaxation time T_0.

Aris, in his method of moment, found out that the rate of change of variance is proportional to the sum of the molecular diffusion coefficient and the Taylor diffusion coefficient. Therefore, according to Aris [2] the rate of growth of variance is defined as:

$$\frac{dv_2}{dt} = 2 + 2\mathrm{Pe}^2 D_*(S, \alpha, T_0, t) \tag{22}$$

where D_* is the apparent dispersion coefficient depending on parameters S, α, T_0 and t. The first term on the right hand side of the above expression represents the longitudinal diffusion, whereas the second term represents the interaction between the convection and lateral diffusion. Therefore, the apparent dispersion coefficient D_* is discussed. Taking $\mathrm{Pe} = S = 10^3$, the variation of D_* against dispersion time t has been presented for various values of T_0 in Fig. 7 for $\alpha = 0.5$ and Fig. 8 for $\alpha = 4.0$. The variation of D_* in oscillatory flow changes cyclically with a double frequency and reaches a stationary state after a certain time, which is related to the cross-sectional mixing time. The amplitudes of oscillation of D_* during the first and second half of a complete period of oscillatory flow are almost symmetrical for low frequency (Fig. 7), whereas for the high frequency parameter, D_* is more significant during the first half of the period than the second one (Fig. 8). However, this situation completely stabilizes after a certain time and then the solute disperses at a fairly uniform rate (Mazumder and Das [6], Yasuda [10]). The apparent dispersion coefficient D_* in the low frequency of oscillation reaches a stationary state earlier than for the high frequency. The dispersion coefficient D_* changes cyclically with time even in the stationary state.

The longitudinal dispersion of solute strongly depends on the visco-elastic parameter T_0. The effect of T_0 for a small value of α is small compared to that for a large value of α. Figure 7(a, b) shows the increment in phase lag of D_* with increase of T_0 due to a decrease of the modulus of elasticity. Initially, at the low frequency of oscillation the amplitude of D_* decreases during the first half of the period of oscillation and then increases in the second half with increase in T_0; at large time [Fig. 7(b)] it becomes stable with the flow. Figure 8(a, b) shows the variation of D_* with time when $\alpha = 4.0$ for different T_0. Initially, a double-frequency oscillation is observed and the difference between two consecutive oscillations increases with increase in α, i.e. increase in frequency of oscillation, and for this it takes a larger time to reach the steady state. The amplitude of the oscillation increases with increase in T_0 which is comparable with the study made by Erdoğan [14] for small values of a non-Newtonian parameter in asymptotically large time.

Once the central moments $v_2, v_3, v_4, \ldots$, are known, it is possible to compute the mean concentration distribution $C_m(t, z)$ deviated from Gaussianity in terms of Hermite polynomial representation (Chatwin [26], Andersson and Berglin [27]) and is given by:

$$C_m(t, z) = M_0(t)e^{-x^2} \sum_{n=0}^{\infty} a_n(t)H_n(x) \tag{23}$$

where

$$M_0(t) = \iiint C \, dv, \quad x = \frac{z - z_g}{(2v_2)^{1/2}}, \quad z_g = \frac{M_1}{M_0}$$

and H_i, the Hermite polynomials, satisfy the recurrence relation with $H_0(x) = 1.0$ as

$$H_{i+1}(x) = 2xH_i(x) - 2iH_{i-1}(x), \quad i = 0, 1, 2, \ldots \tag{24}$$

The coefficients a_i are

$$a_0 = 1/(2\pi v_2)^{1/2}, \quad a_1 = a_2 = 0, \quad a_3 = 2^{1/2}a_0\beta_2/24, \quad a_4 = a_0\beta_3/96.$$

Coefficient of skewness $\beta_2 = v_3/v_2^{3/2}$, and that of kurtosis $\beta_3 = v_4/v_2^2 - 3$ represent the degree of symmetry and peakedness of the distribution of solute respectively. These indicate basically the nature of the distribution and the deviations from Gaussianity. If the distribution is exactly Gaussian, both coefficients will be zero.

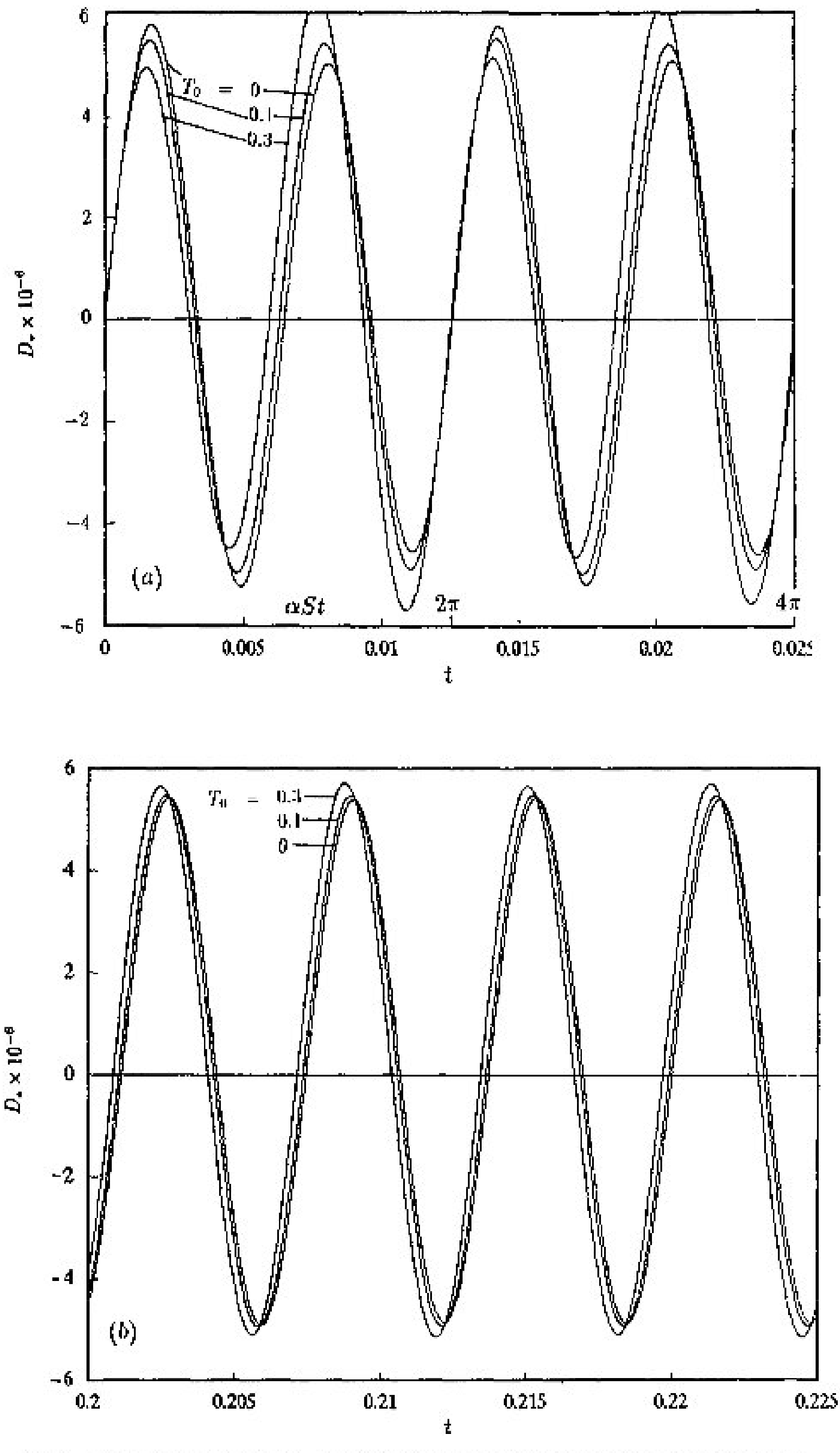

Fig. 7. The dispersion coefficient D_* for (a) small time, (b) large time, when Pe = S = 1000, α = 0.5.

Table 1 shows the variation of β_2 and β_3 with the frequency of oscillation α, viscoelastic parameter T_0 and the dispersion time t. It is seen from the table that there is a small deviation in β_2 from zero, which increases with the increase of T_0. The variation for T_0 becomes oscillatory for large values of α which is clear from the table when $\alpha = 4.0$. β_3

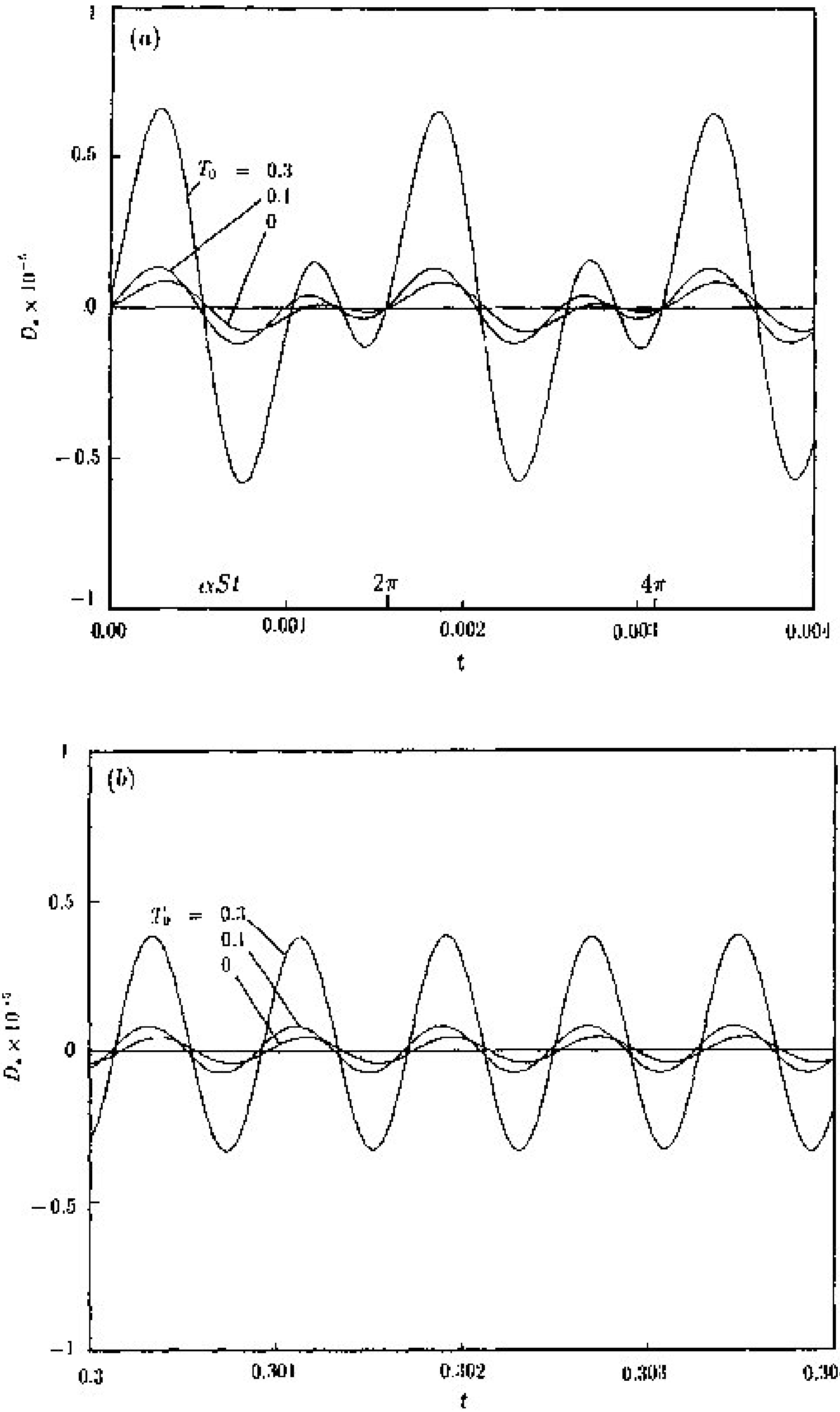

Fig. 8. As Fig. 7 but $\alpha = 4.0$.

increases with increase of T_0 as well as α. With increase of time, β_2 decreases steadily for small α and for large values of α it decreases in oscillatory nature. But β_3 decreases steadily for all α with increase of time t. So it is revealed that if we increase the non-Newtonian parameter, i.e. increase the elastic property in fluid, it takes much time to reach the Gaussianity.

Table 1. Variation of coefficients of skewness (β_2) and kurtosis (β_3)

T_0	t	$\alpha = 0.5$		$\alpha = 4.0$	
		β_2	β_3	β_2	β_3
0.0	0.25	0.00343	− 1.60	0.00041	− 0.011
0.1	0.25	0.00356	0.0025	0.00096	0.0031
0.3	0.25	0.00388	0.0028	0.00734	0.0443
0.3	0.20	0.00444	0.0033	0.01610	0.0514
0.3	0.15	0.00508	0.0040	0.01630	0.0604

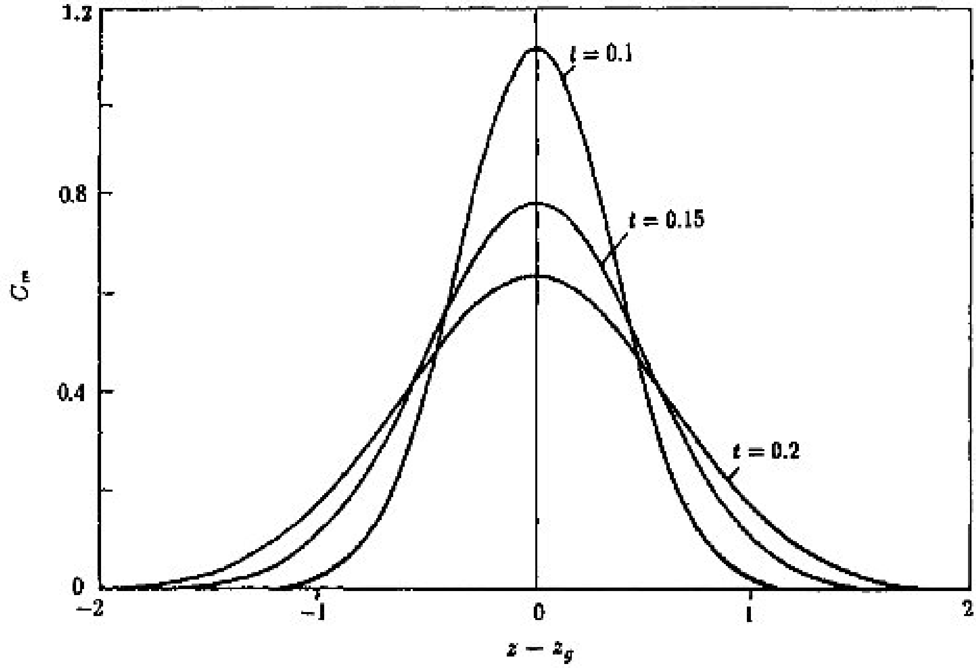

Fig. 9. The mean concentration distribution C_m along the pipe for Pe = S = 1000, $T_0 = 0.3$ and $\alpha = 0.5$.

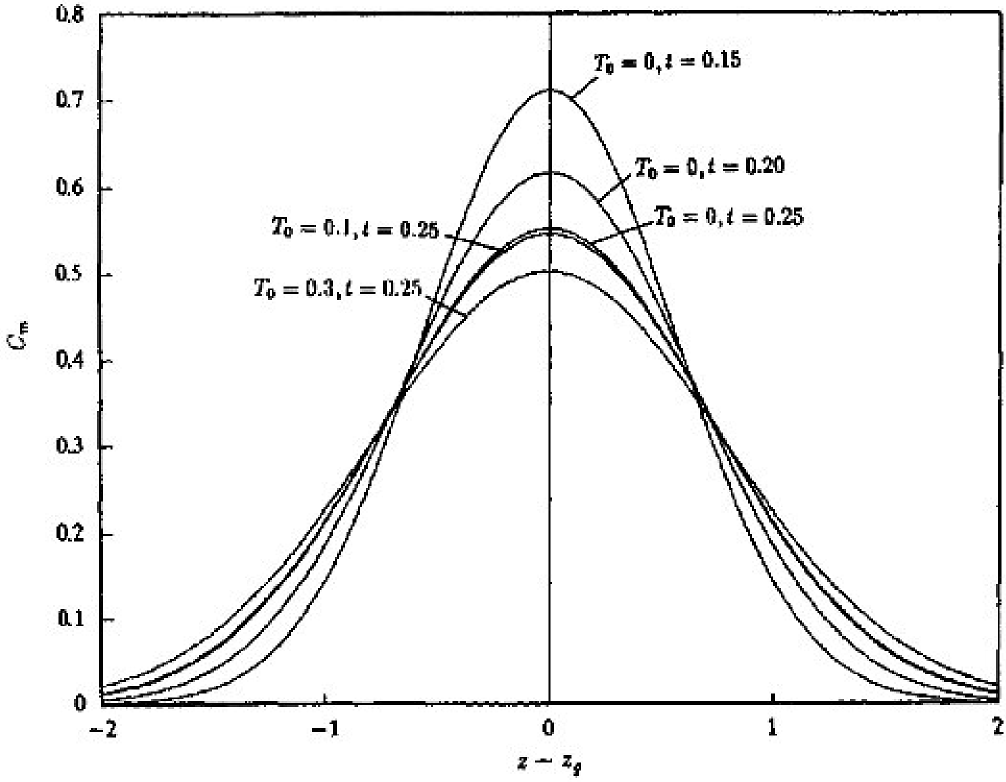

Fig. 10. The mean concentration distribution C_m along the pipe for Pe = S = 1000, and $\alpha = 4.0$.

In Figs 9 and 10, $C_m(t, z)$ has been plotted against axial distance $(z - z_g)$ for different values of time t and T_0 when $\alpha = 0.5$ and 4.0, respectively. From the figures it is observed that the peak of the concentration distribution gradually decreases with increase of dispersion time t as well as increase of relaxation time T_0, which implies the distribution gradually tends to become flat. It is also seen that the mean concentration distribution due to unsteady flow of viscoelastic fluid is essentially symmetrical. From the above observation it is noted that there is a remarkable similarity between the mean concentration distribution of solute in an unsteady non-Newtonian (viscoelastic) fluid and in periodic flow of a Newtonian fluid discussed by Mazumder and Das [6]. Mean concentration distribution profiles show how fast the slug's centre of gravity moves, how it disperses due to shear effects and how the distribution deviates from the Gaussianity due to the viscoelastic parameter.

Acknowledgements—The authors would like to express their sincere thanks to Professor K. R. Rajagopal for his helpful suggestions. One of us (D. C. Dalal) is thankful to the CSIR, India, for financial support for pursuing this work.

REFERENCES

1. G. I. Taylor, *Proc. R. Soc. Lond.* **A219**, 186 (1953).
2. R. Aris, *Proc. R. Soc. Lond.* **A235**, 67 (1956).
3. N. G. Barton, *J. Fluid Mech.* **126**, 205 (1983).
4. R. Aris, *Proc. R. Soc. Lond.* **A259**, 370 (1960).
5. A. Mukherjee and B. S. Mazumder, *Acta Mechanica* **74**, 107 (1988).
6. B. S. Mazumder and S. K. Das, *J. Fluid Mech.* **239**, 523 (1992).
7. P. C. Chatwin, *J. Fluid Mech.* **71**, 513 (1975).
8. R. Smith, *J. Fluid Mech.* **114**, 379 (1982).
9. C. F. Jimenez and P. J. Sullivan, *J. Fluid Mech.* **142**, 57 (1984).
10. H. Yasuda, *J. Fluid Mech.* **148**, 383 (1984).
11. B. S. Mazumder and S. K. Das, *Acta Mechanica* **80**, 151 (1989).
12. L. T. Fan and W. S. Hwang, *Proc. R. Soc. Lond.* **A283**, 576 (1965).
13. L. T. Fan and C. B. Wang, *Proc. R. Soc. Lond.* **A292**, 203 (1966).
14. M. E. Erdoğan, *I & EC Fundamentals* **6**, 463 (1967).
15. S. Ghoshal, *Chem. Engng Sci.* **26**, 185 (1971).
16. S. N. Shah and K. E. Cox, *Chem. Engng Sci.* **29**, 1282 (1974).
17. A. S. Gupta and B. S. Mazumder, *Int. J. Heat Mass Transfer* **20**, 341 (1977).
18. R. S. Subramanian and W. N. Gill, *Can. J. Chem. Engng* **54**, 121 (1976).
19. R. B. Bird, W. E. Stewart and E. N. Lightfoot, *Transport Phenomena*. Wiley, New York (1960).
20. J. G. Oldroyd, *Proc. R. Soc. Lond.* **A200**, 523 (1950).
21. S. Uchida, *Z. Angew. Math. Phys.* **7**, 403 (1956).
22. H. Schlichting, *Boundary-Layer Theory*. McGraw-Hill (1979).
23. E. M. Khabakhapasheva, V. I. Popov, A. N. Kekalov and E. S. Mikhailova, *J. Non-Newtonian Fluid Mech.* 289 (1989).
24. D. W. Beard and K. Walters, *Proc. Camb. Phil. Soc.* **60**, 667 (1964).
25. K. R. Rajagopal and E. Sciubba, *Maths Computers Simulation* **26**, 276 (1984).
26. P. C. Chatwin, *J. Fluid Mech.* **43**, 321 (1970).
27. B. Andersson and T. Berglin, *Proc. R. Soc. Lond.* **A377**, 251 (1981).